JOURNAL OF MATERIALS SCIENCE **39** (2004) 3965–3974

Role of minor alloying additions in formation of bulk metallic glasses: A Review

Z. P. LU*, C. T. LIU
Metals and Ceramic Division, Oak Ridge National Laboratory, TN 37831-6115, USA
**E-mail: luzp@ornl.gov*

Minor alloying addition or microalloying technology has already shown dramatic effects on glass formation and thermal stability of bulk metallic glasses (BMGs). This paper intends to provide a comprehensive review of recent developments of this technology in the field of BMGs. The beneficial effects of minor alloying additions on the glass formation and the thermal stability of BMGs will be summarized and analyzed. In addition, principles and guidelines for future application of this technology will also be proposed.

1. Introduction

The emergence of synthetic bulk metallic glasses (BMGs) as a prominent class of functional and structural materials with a unique combination of properties has been an important part of the materials science scene over the past decade. Compositional dependence of glass-forming ability (GFA) and thermal stability in various systems has been mapped out. As a result, hundreds of bulk glass-forming alloys with diameters up to several centimeters have been identified and prepared [1–3]. However, the engineering commercialization of these BMGs as structural materials is hindered by their limited GFA, low thermal stability and unsatisfactory manufacturability. Recently, limited work has shown that microalloying with certain alloying elements, usually <2 at.%, is a potent approach overcoming these drawbacks. For example, with 0.5 to 1 at.% addition of Si, the attainable maximum thickness of glassy ingots in the Cu-Ti-Zr-Ni system was increased from 4 to 7 mm [4]. Oxygen impurity drastically reduces GFA and embrittles Zr-based alloys, but microalloying with a combination of (0.1% B + 0.2% Si + 0.1% Pb) was found to be extremely effective in overcoming this issue [5]. However, the underlying mechanisms and principles of this technology are still amiss.

Minor alloying additions or microalloying technologies were key metallurgical practices and dominant concepts for developing new metallic crystalline materials in the late half of the 20th century. A prominent example is the invention of ductile intermetallic Ni_3Al alloys. With addition of 0.1 wt% B, the room temperature ductility of Ni_3Al (24 at.% Al) was dramatically increased to 53.8% [6]. Grain boundary segregation and slowdown of hydrogen diffusion were responsible mechanisms in this specific crystalline material. The development of microalloying technologies and their responsible mechanisms for crystalline metallic materials in the 20th century is summarized in Table I [7].

It is our belief that the minor alloying addition technique in the new century will continue playing an important role in the materials science field, as indicated in Table I. In this paper, we intend to summarize recent applications of this technique in BMGs and rationalize its roles in formation of BMGs. Guidelines and future directions for applying this technique in the field of BMGs will also be surmised.

2. Roles of minor alloying additions in the field of BMGs

It was found that appropriate minor alloying additions were very effective in increasing GFA, enhancing thermal stability and improving magnetic and mechanical properties for some BMGs. In this paper, however, we will focus only on the effect of minor alloying (microalloying) additions on GFA and thermal stability of BMGs. We use the attainable thickness (Z_{max}) of glassy alloys and the supercooled liquid region ΔT, defined as the temperature interval between the glass transition temperature T_g and the onset crystallization temperature T_x, to indicate GFA and thermal stability of BMGs, respectively.

2.1. Effects of minor alloying additions on GFA

To date, various elements have been chosen for microalloying in BMGs, and their effects on GFA and thermal stability is summarized in Table II [8–44]. Based on their atomic sizes shown in Fig. 1 [45], these elements can be categorized into three groups: (1) small metalloid elements like C, B, Si, (2) intermediate transition metals such as Fe, Ni, Co, Cu, Mo, Zn, Nb, Ta, Ti, and (3) large elements like Zr, Sn, Sc, Sb, Y, La and Ca. In the following, we will summarize the microalloying effects based on the atomic sizes of alloying elements.

2.1.1. Additions of small atoms

There is no doubt that high oxygen concentration has a detrimental effect on glass formation for BMGs,

TABLE I Development of microalloying technology and corresponding theories in the 20th century [7]. New role of this technology in materials science field is also predicted

Period	Technologies	Mechanisms
1920-	Thoria-Tungsten	Surface Adsorption
	Grain-oriented Si-steel	Nucleation
1940-	Boron steel	Grain boundary pinning
	Nodular graphite cast iron	Grain boundary segregation
1960-	HSLA steel	Solute drag
	Grain-oriented Si-Steel	
1980-	Ductile Ni_3Al	Grain boundary segregation & slowdown of hydrogen diffusion [6]
2000-	Bulk glass formation?	Destabilize the competing crystalline phases?
		Enhance the liquid phase stability?
		Scavenging effect of impurities, e.g., oxygen?

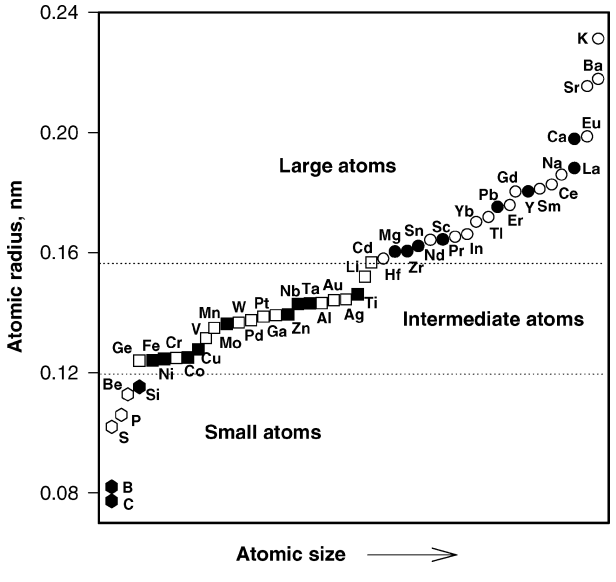

Figure 1 Atomic radius of the possible elements for microalloying in bulk metallic glasses [45]. Solid symbols indicate the elements already used as minor alloying additions.

particularly for Zr-based alloys which have a strong affinity with oxygen [46, 47]. Lin *et al.* [48] clearly demonstrated that oxygen additions dramatically affected the critical cooling rate for glass formation in a Zr-based alloy. In some Zr-based alloys, additions of carbon at ppm levels with/without small doping of the element B could, to a certain degree, alleviate the detrimental effect of oxygen, thereby improving their GFA. However, more than 2% C additions in these alloys induced the formation of Zr carbides, leading to a reduction in the GFA [13].

Boron has been doped in Ni-, La-, Fe- and Zr-based BMGs to promote glass formation [10, 15–19]. For example, in the commercial alloy FC20, an amorphous ingot with 0.5 mm diameter was produced just with 1.5 at.% B addition [16]. For Zr-based alloys, however, their GFA was extremely sensitive to the boron doping level; additions of less than 0.2 at.% B, along with other elements like Pb, C, Si, etc., successfully overcame the harmful effect of oxygen [5]. However, if the boron content exceeded 1 at.%, the formation of Zr borides was stimulated, and the GFA was thus severely deteriorated, although a high concentration boron might be helpful for enhancing the thermal stability of the system (this will be discussed later) [17, 19].

Silicon is effective in facilitating glass formation for refractory-elements-based alloys such as Cu-, Fe- and Ni-alloys [4, 20, 21]. A typical example is its addition in alloy $Cu_{47}Ti_{34}Zr_{11}Ni_8$ (see Table II). Substituting only 1% Ti with Si in this alloy increased its maximum diameter for glass formation from 4 to 7 mm [4]. However, it is very interesting to point out that Si additions of even 1 at.% are extremely detrimental to the GFA of Zr-based alloys due to the formation of silicides [19].

2.1.2. Additions of intermediate atoms

Transitional metals with intermediate atomic sizes, such as Fe, Ni, Co, Cu, Mo, Zn, Nb, Ta and Ti, have been selected as minor alloying elements in various systems. Surprisingly, most of them are detrimental to glass formation [24–32]. Only when their alloying quantities exceed 3 at.% and become a major constituent of the system, have they been shown to be beneficial in bulk glass formation. For example, in order to improve the GFA of alloy $Mg_{65}Cu_{25}Y_{10}$, the addition of Zn has to be at least 5 at.% [28].

2.1.3. Additions of large atoms

Large atoms, such as Zr, Sn, Sc, Y and Pb, are helpful in terms of glass formation [14, 15, 34–42]. Microalloying with 2 at.% Y in Zr- and Fe-based alloys greatly enlarged their attainable maximum sizes for these alloys even with low-purity raw materials. A similar beneficial effect of Sc was observed in a Zr-based alloy [14]. With additions of 300 to 600 ppm Sc, the maximum diameter for glass formation of alloy $Zr_{52.5}Al_{10}Ti_5Cu_{17.9}Ni_{14.6}$ containing 90–120 wppm oxygen was increased from 4.5 to 12 mm. Also, yttrium was found to be able to not only scavenge oxygen from the undercooled liquid but also lower the liquidus temperature in some Fe-based alloys [41, 42]. Tin is extremely effective in promoting glass formation for refractory-elements-based alloys [14, 21, 33–35]. Replacing only 2 at.% of Ni with Sn in alloy $Cu_{47}Ti_{33}Zr_{11}Ni_8Si_1$, for example, increased its maximum size for glass formation by 2 mm [36]. It is to be noticed that some large elements like La, Ca, Sb, etc., have negative effects on the GFA of some Zr- and Ti- based BMGs.

2.2. Effects of minor alloying additions on thermal stability

The quantity $\Delta T (= T_x - T_g)$ is a measure of glass thermal stability which is defined as the resistance of glasses towards devitrification upon reheating above T_g. Thermal stability is of great importance since it determines the processable temperature region for BMGs. As can be seen from Table II, an increasing GFA is not always accompanied by enhanced stability as measured by the

TABLE II Summary of the effects of minor alloying additions in various bulk metallic glasses

Alloying element (M)	Optimum content x (at.%)	Base alloy at.%, unless indicated otherwise	Effect on glass-forming ability increment in Z_{max} (mm) or amorphous volume fraction				Effect on thermal stability $\Delta T(T_x - T_g)$ extension (K)			Ref.
			without	with	Increment	Technique[a]	without	with	Extension	
O	0.4%	$(Zr_{65}Cu_{17.5}Al_{7.5}Ni_{10})_{100-x}M_x$	–	–	Deteriorated	T3	107[h]	94	−13	[8]
	0.8%		–	–	Deteriorated	T3	107[h]	67	−40	[8]
	0.43%	$Zr_{65-x}Cu_{27.5}Al_{7.5}M_x$	–	–	–	–	85[i]	59	−26	[9]
	0.82%		–	–	–	–	85[i]	58	−27	[9]
C	1%	$(La_{55}Al_{25}Ni_{20})_{100-x}M_x$	40%	100%	60%	T2				[10]
	1%	$Zr_{41}Ti_{14}Cu_{12.5}Ni_{10-x}Be_{22.5}M_x$	–	–	Improved[d]	T5	60	90	30	[11, 12]
	2%	$Zr_{41}Ti_{14}Cu_{12.5}Ni_{10-x}Be_{22.5}M_x$	>10	5	−5	T2	61	55	−6	[13]
	0.1%	$(Zr_{52.5}Al_{10}Ti_5Cu_{17.9}Ni_{14.6})_{100-x}M_x$	4.5[g]	5.7	1.2	T6				[14]
B	1–2%	$(La_{55}Al_{25}Ni_{20})_{100-x}M_x$	40%	100%	60%	T2				[10]
	1%	$Ni_{60}Nb_{37-x}Sn_3M_x$	2	3	1	T3	42	58	16	[15]
	1.5%	$FC20(Fe_{81.1}C_{13.8}Si_{5.1})_{100-x}M_x$	0	0.5	0.5	T1				[16]
	4%	$Zr_{65}Cu_{27.5}Al_{7.5-x}M_x$	–	–	–	–	72	100	38	[17]
	3%	$Pd_{76}Cu_6Si_{16-x}M_x$	–	–	–	–	47	70	26	[18]
	1%	$(Zr_{57}Nb_5Cu_{15.5}Ni_{12.5}Al_{10})_{100-x}M_x$	–	–	Deteriorated[e]					[19]
Si	1%	$Cu_{47}Ti_{34-x}Zr_{11}Ni_8M_x$	4	7	3	T1	33	58	25	[4]
	5%	$Ni_{57}Ti_{23-x}Zr_{20}M_x$	0	2	2	T3	17	50	33	[20]
	1%	$Fe_{72}Al_5Ga_2P_{11-x}C_6B_4M_x$	1	2	1	T1	53	55	2	[21]
	1%	$(Zr_{57}Ti_5Cu_{20}Ni_8Al_{10})_{100-x}M_x$	–	–	Deteriorated[e]	T1				[19]
	1%	$(Zr_{57}Nb_5Cu_{15.5}Ni_{12.5}Al_{10})_{100-x}M_x$	–	–	Deteriorated[e]	T1				[19]
	1%	$Ni_{37}Zr_{40}Ti_{23x}M_x$	–	–	Improved	T7	0	25	25	[22]
	2.5%	$Fe_{77}Ga_3P_{12-x}C_4B_4M_x$	0.025	2.5	2.5	T1	28	48	20	[23]
	2.5%	$Fe_{78}Ga_2P_{12-x}C_4B_4M_x$	0.025	2.0	2.0	T1	28	40	12	[23]
	0.1–1%	$(Zr_{52.5}Al_{10}Ti_5Cu_{17.9}Ni_{14.6})_{100-x}M_x$	4.5[g]	1	−3.5	T6				[14]
Fe	2%	$Zr_{41}Ti_{14}Cu_{12.5}Ni_{10-x}M_x$	[b]	[b]	[b]	T2	61	36	25	[24]
	1%	$(Cu_{60}Zr_{30}Ti_{10})_{100-x}M_x$	4	3	−1	T1	38	38	0	[25]
Ni	1%	$(Cu_{60}Zr_{30}Ti_{10})_{100-x}M_x$	4	3	−1	T1	38	44	6	[25]
	3%		4	3	−1	T1	38	53	15	[25]
Co	1%	$(Cu_{60}Zr_{30}Ti_{10})_{100-x}M_x$	4	3	−1	T1	38	43	5	[25]
Cu	2.5%	$Nd_{60-x}Fe_{20}Al_{10}Co_{10}M_x$	3	–	Deteriorated	T1				[26]
Mo	2%	$(Cu_{60}Hf_{25}Ti_{15})_{100-x}M_x$	4	1.5	−2.5	T1	60	40	−20	[27]
Zn	5%	$Mg_{65}Cu_{25-x}Y_{10}M_x$	6	4	2	T3	61	52	−9	[28]
Nb	2.5%	$(Zr_{65}Al_{10}Cu_{15}Ni_{10})_{100-x}M_x$	67%	90%	23%	T4	107	90	−17	[29]
	2%	$Fe_{72-x}Al_5Ga_2P_{11}C_6B_4M_x$			Deteriorated		65	63	−2	[30]
	2%	$Fe_{72}Zr_{10-x}B_{20}M_x$					83.2	91.3	8.1	[31]
	4%	$(Co_{70.5}Fe_{4.5}Si_{10}B_{15})_{100-x}M_x$	0.02	1	1	T1	0	38	38	[32]
	2%	$(Cu_{60}Hf_{25}Ti_{15})_{100-x}M_x$	4	4	0	T1	60	46	−14	[27]
Ta	2%	$(Cu_{60}Hf_{25}Ti_{15})_{100-x}M_x$	4	3.5	−0.5	T1	60	51	−9	[27]
Ti	1%	$Zr_{60}Cu_{20}Ni_{10-x}Al_{10}M_x$	2.1	1.5	−0.6	T6	112	126	14	[33]
	5%		2.1	3.3	1.2	T6	112	69	−43	[33]
Zr	2%	$Co_{40}Fe_{22}Nb_{8-x}B_{30}M_x$	0	1	1	T1	81	98	17	[34]
Sn	3%	$Ni_{60}Nb_{40-x}M_x$	0	2	2	T3	0	42	42	[15]
	1%	$(Cu_{60}Zr_{30}Ti_{10})_{100-x}M_x$	4	5	1	T1	37	46	9	[35]
	2%	$Cu_{47}Ti_{33}Zr_{11}Ni_{8-x}Si_1M_x$	4	6	2	T3	37	45	8	[36]
	3 wt%	$(Zr_{52.5}Ti_5Al_{10}Ni_{14.6}Cu_{17.9})_{100-x}Sn_x$	–	–	–	–	62	91	29	[37]
	1%	$Ni_{57}Zr_{20}Ti_{23-x}M_x$				T7	0	23	23	[22]
Sc	0.03–0.06%	$(Zr_{52.5}Al_{10}Ti_5Cu_{17.9}Ni_{14.6})_{100-x}M_x$	4.5[g]	12	7.5	T6	41	48	7	[14]
Sb	1%	$Ti_{50}Cu_{25}Ni_{25-x}M_x$	–	–	–	–	40	33	−7	[38]
Y	2–4%	f	0[f]	5	5	T1	62	100	38	[39]
	2%	$(Cu_{60}Zr_{30}Ti_{10})_{100-x}M_x$	4	5	1	T1	37	50	13	[40]
	1.5–2%	$Fe_{63-x}Zr_8Co_6Al_1Mo_7B_{15}M_x$	1.5	5	3.5	T1	76	64	−12	[41, 42]
	1.5–2%	$Fe_{63-x}Zr_8Co_5Cr_2Mo_7B_{15}M_x$	1.5	5	3.5	T1	76	61	−15	[41, 42]
La	0.1–1.0%	$(Zr_{52.5}Al_{10}Ti_5Cu_{17.9}Ni_{14.6})_{100-x}M_x$	4.5[g]	1	−3.5	T6				[14]
Ca	0.3%	$(Zr_{52.5}Al_{10}Ti_5Cu_{17.9}Ni_{14.6})_{100-x}M_x$	4.5[g]	2	−2.5	T6				[14]
Mixture	0.1B + 0.2Si + 0.1Pb	$(Zr_{52.5}Al_{10}Ti_5Cu_{17.9}Ni_{14.6})_{100-x}M_x$	0[f]	6.4	6.4	T1				[5]
	0.6 Mix[c]	$Fe_{61}Co_7Zr_{10}Mo_5W_2B_{15}M_x$	0[f]	2	2	T1	–	–	7	[43]
	1%Y + 0.5%Mg	$Zr_{41}Ti_{14}Cu_{12.5}Ni_{10-x}Be_{22.5}M_x$	>10	5	< −5	T2	61	44	−17	[13]
	0.2%B + 0.2%C	$(Zr_{52.5}Al_{10}Ti_5Cu_{17.9}Ni_{14.6})_{100-x}M_x$	0[f]	6.2	6.2	T1			0	[44]

Notes:

[a]T1: copper mold casting; T2: water quenching; T3: injection copper mold casting; T4: arc-melting; T5: solidified at very low cooling rates; T6: suction casting with wedge-shaped mold, T7: melt-spinning.

[b]No appreciable difference.

[c]Mix: a mixture of elements including B, Al, Si, C and P.

[d]All alloys solidified at very low cooling rates, and the alloys with carbon additions showed a larger volume fraction of amorphous phase than those without carbon.

[e]with 1 at.% Si addition, as-cast, 5 mm rods lost their glass nature, and crystalline phases like silicides were formed.

[f]Low impurity raw materials.

[g]Oxygen content is about 90–120 wppm.

[h]Oxygen content is about 0.2 at.%.

[I]Oxygen content is 0.14 at.%.

supercooled liquid region ΔT. This is consistent with our previous observation for BMGs [49].

Oxygen effects on crystallization in Zr-based alloys have been well studied [8, 9, 46, 47, 50]. It was found that high oxygen content induced the precipitation of metastable quasicrystalline phases in these alloys and, in turn, significantly destabilized the supercooled liquid, i.e., drastically decreased the ΔT values.

Carbon can increase the thermal stability of Zr-based BMGs, for example, 1 at.% C addition extended the supercooled liquid region of alloy $Zr_{41}Ti_{14}Cu_{12.5}Ni_{10}Be_{22.5}$ by 30 K. Similar to its effect on GFA, more than 1% C (e.g., 2%, see Ref. [13]) in this alloy started to destabilize the supercooled liquid. Boron additions have successfully enlarged the supercooled liquid regions by 38 and 26 K, respectively, for $Zr_{65}Cu_{27.5}Al_{7.5}$ [17] and $Pd_{76}Cu_6Si_{16}$ [18]. More boron additions in both alloys also caused a decrement in ΔT values because boron initiated the formation of more stable crystalline phases. Silicon can enhance the thermal stability in various refractory-elements-based systems [4, 20–23]. For example, with addition of 1 at.% Si in alloy $Cu_{47}Ti_{34}Zr_{11}Ni_8$, the crystallization peak shifted to a higher temperature but the glass transition temperature remained unchanged. Consequently, the supercooled liquid region was largely extended [4].

The effects of microalloying with transitional metals having intermediate atomic sizes on the thermal stability changed from system to system. In some systems like Zr-based alloys, thermal stability was greatly increased with small additions. However, their additions in most BMGs usually deteriorated the GFA (see Table II). This also indicates that the GFA and thermal stability are different properties of BMGs.

Large atoms like Zr and Sn are very effective in enlarging the supercooled liquid region for BMGs. The main reason is that their additions suppress the precipitation of crystalline phases during reheating of the glasses. For example, in $Co_{40}Fe_{22}Nb_8B_{30}$, replacing 1 at.% Nb with Zr destabilized the phase of $Co_{21}Nb_2B_6$ and changed the crystallization mode of this alloy from two stages to a single stage, thus expanding the supercooled liquid region [34].

3. Discussion

3.1. Origins of improved GFA

As discussed in references 49 and 51, glass formation is always a competing process between molten liquid and crystalline phases. The GFA of BMGs is related to two aspects: (1) liquid phase stability, and (2) the stability of competing crystalline phases. Either increasing the liquid phase stability or destabilizing the competing crystalline phases can increase the GFA of glass-forming liquids. Next, we will analyze the underlying mechanisms of GFA improvement via microalloying.

3.1.1. Additions of large atoms

Additions of large atoms in a system increase the atomic size mismatches among all constituents. Based on one of the so-called Hume-Rothery rules [52], the solubility of these added large atoms in the competing crystalline phases containing one or a plurality of major constituents is likely restricted. In molten liquids, small amounts of these large atoms can be dissolved homogeneously. But during the crystallization process upon cooling, these atoms have to be redistributed (i.e., long-range inter-diffusions are required) due to their limited solubility in the competing crystalline phases. Meantime, according to the theory of cohesion in metals [53], large atoms usually have a large negative heat of mixing with other small or intermediate atoms (i.e., the atomic bonding between these elements are typically strong). As a result, they have a high tendency to form compounds instead of solid solutions. In the following, the beneficial effects of the additions of large atoms on glass formation are summarized.

3.1.1.1. Destabilize the competing crystalline phases. Due to their limited solubility, the added large atoms have to be redistributed during the crystallization process upon cooling. Firstly, the additions of these atoms make it difficult for the concentrations of all elements to simultaneously satisfy the composition requirements of the crystalline nucleus. This is because long-range rearrangement of more kinds of atoms is involved. Secondly, rejecting these large atoms from the crystalline nucleus changes the composition and interfacial energy at the solid/liquid interface. In addition, necessary long-range inter-diffusions slow down the subsequent crystal growth rate of the nucleus. All of these contributions suppress the formation and growth of the competing crystalline phases. In turn, the glass formation is promoted.

3.1.1.2. Stabilize the liquid phase. Firstly, due to their low solubility in the competing crystalline phases, additions of these large atoms in off-eutectic alloys tend to effectively suppress the formation of the competing crystalline phases (i.e., primary phases in these cases) and adjust the composition close to the eutectic, thereby lowering the melting point (i.e., the liquid phase is stabilized). Secondly, as mentioned earlier, large elements generally have a high tendency of compound formation with major constituents in a base alloy [52, 53], which increases its short-range compositional ordering and favors the formation of clusters in the undercooled liquid. It was experimentally confirmed that the local chemical configuration of the clusters in undercooled liquids was extremely different from that of the long-range crystalline ordering [2, 54–56]. In order to form crystalline structure, the atomic pairs in these clusters have to be broken apart upon cooling to form new, stronger chemical bonds with the other constituents. The frustration between the short-range bond ordering and the long-range crystalline ordering actually controls, to some extent, the fragility and the GFA of the undercooled liquids [57]. As such, a stronger chemical short-range ordering due to the additions of the large atoms tends to enhance the liquid phase stability and, in turn, retards the crystallization process.

It was found that microalloying with Y in several Cu- and Fe-based alloys can greatly improve their GFA

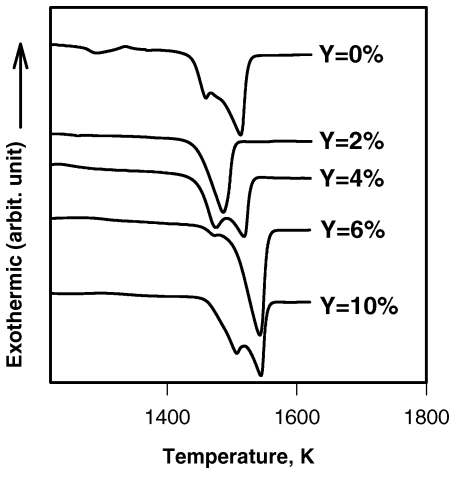

Figure 2 Melting curves for alloys $Fe_{63-x}Y_xZr_8Co_6Al_1Mo_7B_{15}$ (x = 0, 2, 4, 6 and 10 at.%) with various yttrium contents, obtained by a differential scanning calorimeter (DSC) at a heating rate of 20 K/min [42].

via lowering their liquidus temperatures [40–42]. As shown in Table II, replacing 2 at.% Fe with Y in alloy $Fe_{63}Zr_8Co_6Al_1Mo_7B_{15}$ increased the maximum size for glass formation from 1.5 to 5 mm. The melting curves for alloys $Fe_{63-x}Y_xZr_8Co_6Al_1Mo_7B_{15}$ (x = 0, 2, 4, 6 and 10 at.%) with various yttrium contents, obtained by a differential scanning calorimeter (DSC) at a heating rate of 20 K/min, are plotted in Fig. 2. With no yttrium addition, the alloy exhibits an incipient melting, followed by two endothermic peaks corresponding to extensive melting events for this alloy. The first peak of the extensive melting in this alloy is due to the eutectic melting, and the second peak is ascribed to the melting of the α-Fe phase. With addition of 2% Y, the second peak due to the melting of the α-Fe phase almost disappears. As a result, the offset temperature (liquidus temperature) is reduced by $\sim$25 K. However, with further increase of yttrium to 4% or more, the melting curve re-splits into two peaks, and the liquidus temperature is raised about 30 K. This clearly demonstrates that the appropriate amount of yttrium addition in this alloy can decrease the liquidus temperature greatly, which is mainly due to the facts that, (1) yttrium has the largest atomic size among all constituents in this alloy and a resulting low solubility in α-Fe (i.e., $<$0.6 at.% at 1350°C) and (2) Y has a higher tendency to form compounds with B compared with Fe (heats of mixing for Y-B and Fe-B are -35 and -11 kJ/mol, respectively, see Ref. [53]).

Similar results were observed in alloy $Cu_{47}Ti_{33}Zr_{11}Ni_8Si_1$ by Park *et al.* [36]. Substituting only 2% Ni by Sn lowered the liquidus temperature by 140 K. A large atomic size difference between Sn and the other constituent elements is favorable to destabilize the competing crystalline phases (i.e., the primary phases) and adjust the composition to the eutectic because of the limited solubility of Sn in the primary phases. The larger negative heat of mixing between Sn and other constituent elements, compared to those between Ni and other constituent elements, can contribute to the stabilization of the liquid phase by changing the local atomic structure.

However, excessive additions of the large atoms can induce compound formation and destroy the original randomly packed structure, thus moving the composition away from the eutectics along other directions (i.e., the compounds become the new primary phases). As a result, the liquidus temperature is increased and the GFA is decreased. In the Fe-based alloys mentioned above, the addition of more than 2 at% Y induced the formation of $Fe_{17}Y_2$ phase and raised the melting point to higher temperatures. The same phenomenon was observed in the aforementioned Cu-based system, the melting point was increased from 1140 K for the alloy with 2% Sn to 1322 K for the alloy with 8% Sn.

3.1.2. Additions of small atoms

Metalloid elements such as C, B and Si have strong tendency to form compounds with most metallic elements [52, 53], and their atomic sizes are on the small side (see Fig. 1). Similar to the large atoms, small amounts of their additions also increase the atomic size mismatches among all constituents. Thus, their solubility in the competing crystalline phases consisting of one or a plurality of major constituents is also restricted based on the Hume-Rothery rules. In this regard, their effects on glass formation are similar to those of large atoms discussed previously. Additionally, small atoms can easily occupy interstitial free spaces (i.e., crystallographic holes) and tighten the packed structure of undercooled liquids, which lowers the free energy and stabilizes the liquid phase. In the following, we sum up the effects of these small atoms on glass formation.

3.1.2.1. Destabilize the competing crystalline phases. Due to their limited solubility in the competing crystalline phases, long-range redistribution of these extra small atoms is necessary during the crystallization process upon undercooling. Inevitably, a high concentration layer of these atoms ahead of the solid/liquid interface is built up. Such a buildup definitely retards the nucleation process. Also, the limited solubility of the small atoms in the competing crystalline phases hinders their growth, thus retarding their formation.

3.1.2.2. Stabilize the liquid phase. Small atoms can occupy interstitial spaces among the major constituent atoms, thus increasing the packing density of the liquids. Meantime, due to their strong atomic bonding with metallic elements (i.e., high tendency for forming compounds), additions of small metalloid atoms can enhance the short-range compositional order of glass-forming liquids. As such, the liquid phase stability is heightened. In addition, similar to the large atoms, these small metalloid atoms can also suppress the formation of the competing crystalline phases (i.e., primary phases) in off-eutectic compositions and adjust the composition close to the eutectic. Consequently, the melting point of the resulting alloy is lowered (i.e., the undercooled liquid is stabilized [51]).

However, too much of these small atoms can decrease the GFA. This deterioration can be ascribed to two causes. Firstly, excessive additions stimulate

the formation of new, more stable competing crystalline phases. For example, addition of 1% C in $Zr_{41}Ti_{14}Cu_{12.5}Ni_{10}Be_{22.5}$ greatly improved its GFA, whilst addition of >2 at.% C induced the formation of new stable competing crystalline phases (e.g., Zr carbides), thus demoting the glass formation [13]. The other cause is presumably that the highly packed structure of glass-forming liquids is disturbed if the added amount of these small atoms exceeds the total number of available interstitial sites, thus leading to the worsening of the GFA.

As an example, in the system $Fe_{77}Ga_3P_{12}C_4B_4$, substituting 2.5% P with Si suppressed the formation of the primary phase (i.e., destabilized the primary phase via the solubility limitation) and decreased the melting point by 50 K. As a result, the maximum size for glass formation was increased 100 times (i.e., from 25 to 2.5 mm). However, further increase of Si demoted the glass formation because Si stimulated the formation of the α-Fe phase [23].

3.1.3. Additions of intermediate size atoms

Microalloying with transitional metals having intermediate atomic sizes seemed to be less effective on glass formation. Based on the Hume-Rothery rules, they tend to form solid solutions with other constituents during solidification. Thus, their small additions have less impact on the GFA because of the marginal atomic size mismatches among all constituents and the high tendency of solid-solution formation. In alloy $Nd_{60}Fe_{20}Al_{10}Co_{10}$, for example, replacing 2.5% Nd with Cu actually degraded its GFA. This degradation can be ascribed to: (1) the marginal mismatches of atomic sizes between Fe, Al, Co and Cu, and (2) the high tendency of forming solid solutions between Fe, or Co and Cu.

3.1.4. Additions of crystallization anticatalysts

It is well known that the glass formation in some BMGs like Zr- and Fe-based alloys are very sensitive to oxygen impurity; as a result, high-purity, high-cost materials have to be used for manufacturing. Minor alloying addition technology is a promising approach to alleviate such harmful effects of oxygen. As a typical example, Liu *et al*. [5] has added a mixture of 0.1% B, 0.2% Si and 0.1% Pb to a Zr-based alloy $Zr_{52.5}Al_{10}Ti_5Cu_{17.9}Ni_{14.6}$ that contained about 3000 appm oxygen, and successfully overcame the detrimental effect of oxygen on glass formation, as shown in Fig. 3. Without dopants, the as-cast alloy (6.4 mm in diameter) showed a typical crystalline structure. On the contrary, with the optimum dopants the alloy displayed mostly a single amorphous phase. The beneficial effect of the dopants in these alloys can be easily understood by the sketch shown in Fig. 4. In both alloys, tiny Zr_4Ni_2O particles are formed; however, in the microalloyed material, these particles do not trigger the formation of large crystalline phases around them (i.e., do not act as crystallization catalyzing oxides). It was suggested that two factors may

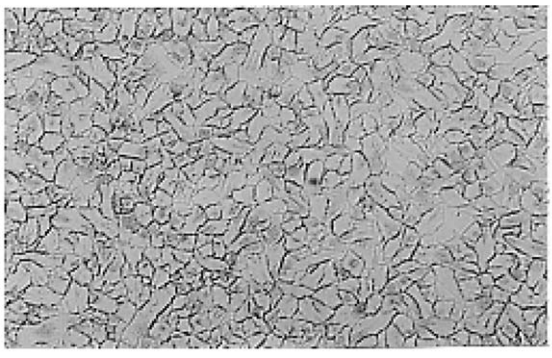

(a): no dopants

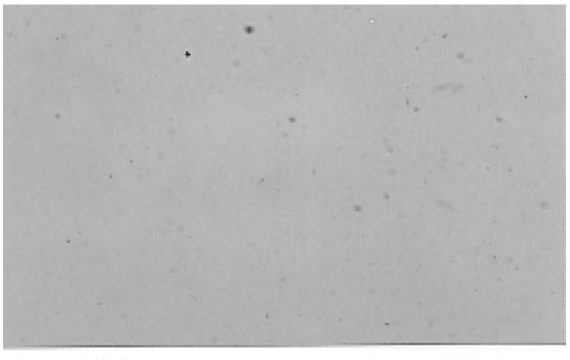

(b): with 0.1% B +0.2% Si + 0.1% Pb

Figure 3 Micrographs of as-cast, 6.4 mm rods of alloy $Zr_{52.5}Al_{10}Ti_5Cu_{17.5}Ni_{14.6}$ with (a) and without (b) dopants of 0.1% B + 0.25% Si + 0.1% Pb [5].

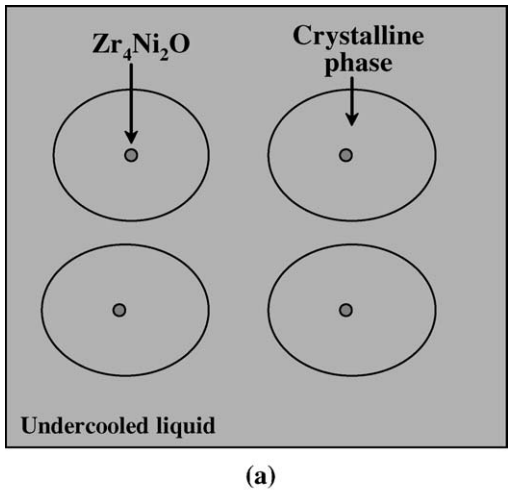

(a)

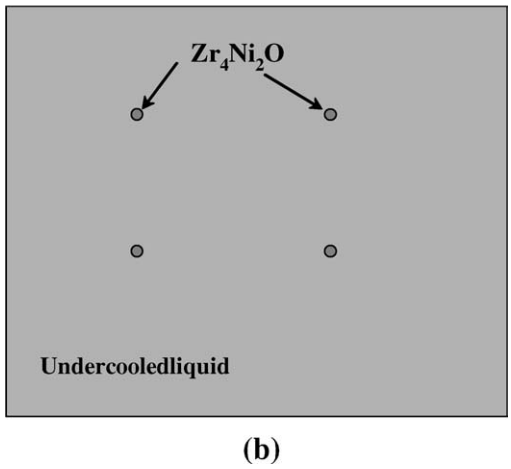

(b)

Figure 4 Sketch to show the beneficial effect of the optimum dopants: (a) no dopants and (b) with the optimum dopants [5].

contribute to this difference. One is that the segregation of the dopants on Zr_4Ni_2O interfaces may change interfacial structures and chemical compositions, thus resulting in suppression of the formation of crystalline phases. The other is that the dopants strongly stabilize the glass matrix phase containing oxygen to the point where the Zr_4Ni_2O particles no longer trigger crystallization of the metallic glass. Similar results in other Zr-based alloys were reported using Sc, Y, C, etc., as crystallization anticatalysts [14, 39].

The current authors also found that Y could effectively neutralize oxygen in the undercooled liquid of Fe-based alloys [41, 42]. As such, the GFA of these alloys was greatly improved. Back-scattered electron microprobe micrographs for the central part of 5 mm drop-cast samples for alloys (a) $Fe_{63}Zr_8Co_6Al_1Mo_7B_{15}$ and (b) $Fe_{61}Y_2Zr_8Co_6Al_1Mo_7B_{15}$ are shown in Fig. 5. Without the addition of yttrium (Fig. 5a), alloy $Fe_{63}Zr_8Co_6Al_1Mo_7B_{15}$ shows typical dendrite phases (dark phase) embedded in the amorphous matrix. For the alloys containing yttrium, only a few spherical particles embedded in the amorphous matrix were seen, as shown in Fig. 5b. These observations obviously demonstrated the beneficial effect of yttrium addition on glass formation. The dark particles in Fig. 5b were identified as yttrium oxides. The average content of oxygen in the amorphous matrix was determined to be around 1038 ± 396 appm. However, for the alloys without Y addition, the oxygen was found to distribute almost evenly over the whole sample and its content averaged as high as 6382 ± 592 appm. Therefore, it can be speculated that, in the molten liquid, little of the yttrium neutralized with the oxygen during the melting and casting processes. The content of oxygen in the remaining liquid was much decreased due to the scavenging effect from yttrium. In addition, the yttrium oxides did not act as heterogeneous nucleation sites, which was presumably ascribed to their crystallographic structures, sizes (too small or too large to be the crystallization catalyst), dispersion and wetting behavior between solid/liquid interfaces. Thus, the remaining liquid was stabilized because of the alleviation of the harmful effect of oxygen, and thereby enabling the formation of glass matrix. This speculation is reasonable because, from a thermodynamic point of view, yttrium has a stronger affinity for the oxygen atom compared with the other elements in the system. The heat of formation of yttrium oxide is 1903.6 KJ/mol, the highest among all oxides of constituent elements (Fe_2O_3, 820.5 kJ/mol; ZrO, 1102.3 kJ/mol; MoO_3, 744.5 kJ/mol; Cr_2O_3, 1128.6 kJ/mol) [58]. The reaction between Y and O is thermodynamically favored compared to the reaction between O and the other elements in the system. Note that the micro-mechanisms underlying the above-mentioned two approaches are slightly different.

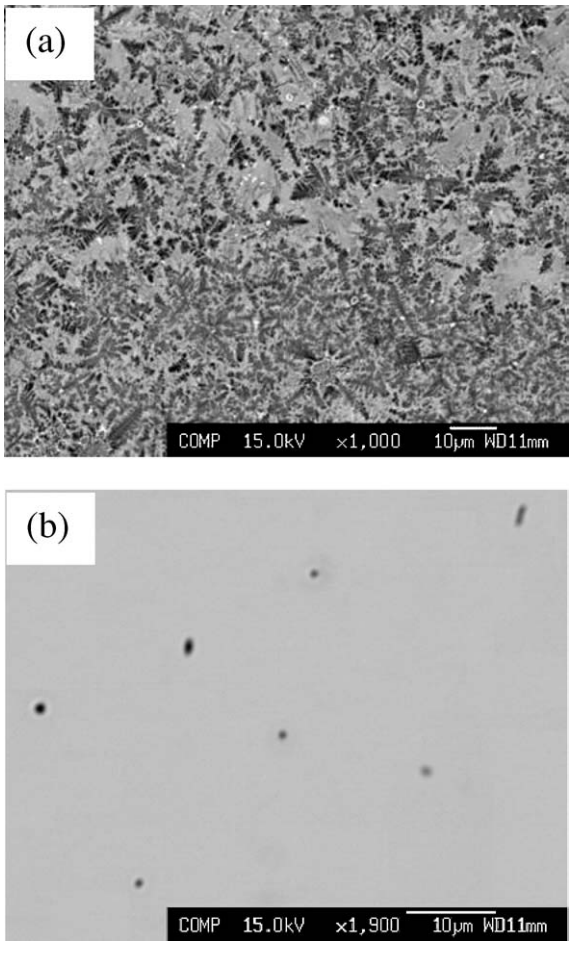

Figure 5 Back-scattered electron microprobe micrographs for the central part of 5 mm drop-cast samples for alloys: (a) $Fe_{63}Zr_8Co_6Al_1Mo_7B_{15}$ and (b) $Fe_{61}Y_2Zr_8Co_6Al_1Mo_7B_{15}$, clearly demonstrating the yttrium effect on glass formation [41].

Microalloying with certain elements to eliminate the side effect of oxygen is a promising approach to improve the manufacturability and GFA of BMGs, hence leading to a lower production cost. It is important to point out that the optimum amount of minor alloying additions strongly depends on the original oxygen level in base alloys. Therefore, from a microalloying technological point of view, the GFA of glass-forming liquids can be enhanced by the following considerations:

(a) choose additional elements having large atomic mismatches with the major constituents;
(b) select elements having high tendency of compound formation (e.g., negative heat of mixing); and
(c) minimize oxygen impurity via microalloying with certain elements.

3.2. The origins of enhanced thermal stability

Thermal stability is measured during reheating of a glass, and the crystalline phases which precipitate first from the amorphous matrix determine the thermal stability of BMGs. Similar to the GFA improvement, how to suppress the nucleation and growth of these crystalline phases during heating is the key to enhancing the thermal stability.

By summarizing the data in Table I, microalloying mechanisms of the thermal stability enhancement can be categorized into three groups described below. The concomitant change in DSC measurements after microalloying is schematically shown in Fig. 6 which clearly demonstrates three types of thermal

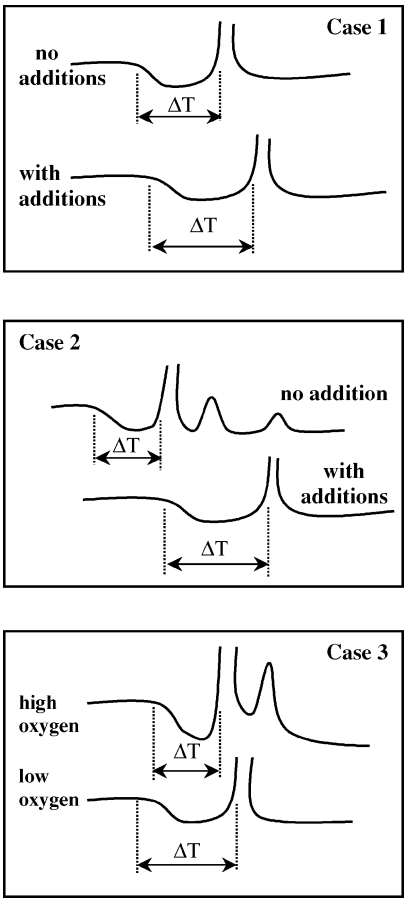

Figure 6 Schematic plot showing the change in DSC measurements after microalloying clearly demonstrating three types of thermal stability enhancement and the responsible micro-mechanisms.

stability enhancement and the responsible microalloying mechanisms.

3.2.1. Increasing the difficulty in atomic rearrangements (single-stage crystallization)

Some of the BMGs crystallize during reheating in one single stage (one peak for the crystallization event in DSC continuous heating curves), i.e., all final crystalline phases precipitate simultaneously out of the matrix. Additions of adequate elements in these alloys do not change the crystallization mode (i.e., still one peak in DSC curve) but they can either induce the formation of extra new phases for the final crystallization product or be preferentially dissolved in certain phases. In both cases, the rearrangement of atoms in the microalloyed alloys becomes much more difficult because more atoms are required to inter-diffuse during reheating. Therefore, the crystallization events are shifted to higher temperatures, thus enlarging the supercooled liquid region (see case 1 in Fig. 6).

For example, with no addition of B, alloy $Zr_{65}Cu_{27.5}Al_{7.5}$ crystallizes in one stage and the crystallized structure consists of Zr_2Cu, Zr_2Al and Zr_5Al_3. With the addition of 4% B, the crystallization mode does not change and all crystalline phases still precipitated simultaneously, but two more phases ZrB_2 and Zr_3Al are observed in the final products. Consequently, more long-range atomic redistribution is necessary, resulting in an extension of 28 K for the supercooled liquid region [17]. Similar results were reported in a Pd-Cu-Si alloy [18]. However, addition of too much B induces the precipitation of even more stable primary phases and changes the crystallization mode, thereby the thermal stability is degraded.

On the other hand, in $Fe_{77}Ga_3P_{12}C_4B_4$ alloy [23], replacing 2.5% P with Si does not change the crystallization mode and the final products that include α-Fe, Fe_3P, Fe_3B and Fe_3C. No new compound containing Si as a constituent element is observed. Si is preferentially dissolved into the Fe_3P phase, and the precipitation of the $Fe_3(P,Si)$ phase becomes more difficult due to the need for the rearrangements of these two kinds of metalloid elements, i.e., P and Si, compared to that of pure Fe_3P phase. As a result, the supercooled liquid region is extended about 20 K [23].

3.2.2. Eliminating the formation of metastable phase during crystallization (multiple-stage crystallization)

Some BMGs crystallize in multiple stages (i.e., multiple peaks appear in their DSC scans). Small additions of proper elements can suppress the phase formation corresponding to DSC peaks at low temperatures and change their crystallization modes to the single-stage, thus enhancing their thermal stability (see case 2 in Fig. 6). For example, amorphous alloy $Ni_{57}Ti_{23}Zr_{20}$ was found to crystallize in the following sequence [20]:

$$\begin{aligned}\text{Amorphous phase} &\rightarrow \text{cubic Ni(Ti, Zr)} \\ &+ \text{remaining amorphous} \\ &\rightarrow \text{orthorhombic } Ni_{10}(Zr, Ti)_7 + \text{cubic Ni(Ti, Zr)}.\end{aligned}$$

Substituting a few percent of Ti with Si, the formation of cubic Ni(Ti, Zr) was suppressed because the Ni(Ti, Zr) phase has very limited solubility for Si and thus long-range redistribution of Si became necessary. The intermediate stage of the crystallization was thus skipped, and only one crystallization peak in DSC curves at a higher temperature was seen. The ΔT value for the microalloyed glass was increased by more than 20 K [20].

3.2.3. Decreasing the oxygen impurity concentration

It was found that oxygen impurities in BMGs changed their crystallization modes and led to the formation of metastable crystallization products (e.g., quasicrystalline phases), and thus lowering their thermal stability significantly (see case 3 in Fig. 6). In alloy $Zr_{65}Al_{7.5}Cu_{17.5}$, for instance, ΔT values increased by 40 K as the oxygen impurity dropped from 0.8 to 0.2 at.% [8]. As discussed earlier, minor alloying additions can scavenge the oxygen from the glass matrix; in turn, it can enhance the thermal stability of BMGs.

As discussed above, in principle, the three guidelines for improving the GFA of BMGs with the minor alloying addition technology also serve to enhance

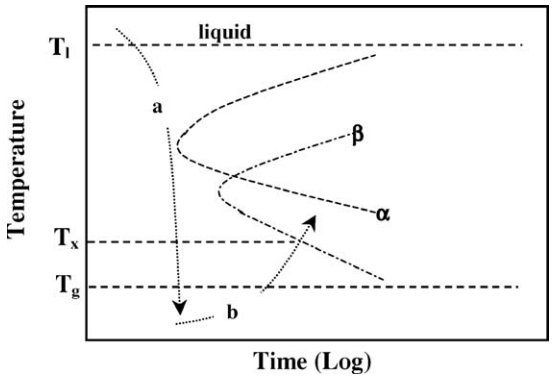

Figure 7 Schematic transformation-time-temperature (TTT) curve showing equilibrium α and non-equilibrium β phases. (a) during cooling to form a glass crystallization of α must be avoided; (b) reheating the glass generally produces β.

the thermal stability of BMGs. However, the micromechanisms of its effects on the GFA and the thermal stability are slightly different, which can be explained by a simple example shown in Fig. 7 illustrating a schematic transformation-time-temperature (TTT) curve of a glass-forming liquid. Below the liquidus temperature T_l, the undercooled liquid crystallizes to the equilibrium phase, α, whilst at lower temperatures a second, metastable phase β can form. During cooling to form a glass, crystallization of α must be avoided, while heat treatment of the glass generally produces β. For such a system, microalloying may be able to suppress the formation of the phase α and improve the GFA, but might not be able to destabilize the β phase and enhance the thermal stability simultaneously. Vice versa, it is also true. Therefore in such kinds of systems, microalloying technology sometimes may show contrasting effects on the GFA and the thermal stability.

It is worth mentioning that the contributing factors to the GFA and the thermal stability of BMGs are related but not completely dependent properties, and all of them should be carefully considered when using microalloying technology. Nevertheless, the solubility limitation still seems to be a critical factor in terms of controlling thermal stability. In addition, the single-stage crystallization mode (i.e., one crystallization peak in DSC heating curves) is an important factor for the achievement of large thermal stability in BMGs, as suggested by Inoue *et al.* [23, 59]. However, based on our analyses, it might not be necessary for obtaining bulk glass formation in some systems. Recent findings in bulk La- [60] and Fe- [41, 42] based glassy alloys has proved this point; the best glass former actually showed multiple crystallization peaks during reheating.

4. Conclusions

1) Minor-alloy addition technology will continue playing critical roles in tailoring the GFA, manufacturability and thermal stability of BMGs.

2) The beneficial effect of microalloying technology on the GFA and the thermal stability of glass-forming alloys include:

1. scavenging the oxygen impurity from the undercooled liquid;
2. destabilizing the competing crystalline phases as results of solubility limitation and slowdown of nucleation and crystal growth processes; and
3. stabilizing the liquid phase via lowering the melting point, enhancing its short-range compositional order, and/or increasing the density of the randomly packed structure of the liquids (small atoms only).

3) The guidelines for the future application of microalloying technology are:

1. choose alloying elements having large atomic size mismatches with the major components;
2. minimize the oxygen impurity via the scavenging effect from certain elements; and
3. select elements having high tendency of compound formation (Note that GFA will be deteriorated if the compound formation becomes dominant).

4) Thermal stability enhancement of metallic glasses can be divided into three types based on the micromechanisms.

5) GFA and thermal stability of metallic glasses are different properties, and minor alloying additions can show contrasting results in a given system.

Acknowledgements

This work was sponsored by the Division of Materials Sciences and Engineering, Office of Basic Energy Sciences (LLH), U.S. Department of Energy under contract DE-AC05-00OR-22725 with UT-Battelle, LLC.

References

1. A. INOUE, in "Bulk Amorphous Alloys: Practical Characteristics and Applications," Materials Science Foundations 6, edited by M. Magini and F. H. Wohlbier (Trans Tech Publications Inc., Swizerland, 1999).
2. *Idem.*, in "Bulk Amorphous Alloys: Preparation and Fundamental Characteristics," Materials Science Foundations 4, edited by M. Magini and F. H. Wohlbier (Trans Tech Publications Inc., Swizerland, 1998).
3. W. L. JOHNSON, *MRS Bull.* **24** (1999) 42.
4. H. CHOI-YIM, R. BUSCH and W. L. JOHNSON, *J. Appl. Phys.* **83** (1998) 7993.
5. C. T. LIU, M. F. CHISHOLM and M. K. MILLER, *Intermetallics* **10** (2002) 1105.
6. C. T. LIU, C. L. WHITE and J. A. HORTON, *Acta. Mater.* **33** (1985) 213.
7. T. NISHIZAWA, *Mater. Trans.* **42** (2001) 2027.
8. J. ECKERT, M. MATTERN, M. ZINKEVITCH and M. SEIDEL, *Mater. Trans. JIM* **39** (1998) 623.
9. B. S. MURTY, D. H. PING, K. HONO and A. INOUE, *Acta. Mater.* **48** (2000) 3985.
10. K. OZAKI, K. KOBAYASHI and T. NISHIO, *Mater. Trans. JIM* **39** (1998) 499.
11. W. H. WANG and H. Y. BAI, *J. Appl. Phys.* **84** (1998) 5961.
12. W. H. WANG, Q. WEI and H. Y. BAI, *Appl. Phys. Lett.* **71** (1997) 58.
13. Y. ZHANG, D. Q. ZHAO, M. X. PAN and W. H. WANG, *J. Non-Cryst. Solids* **315** (2003) 206.
14. A. A. KUNDIG *et al.*, *Mater. Trans.* **43** (2002) 3206.
15. H. CHOI-YIM, D. XU and W. L. JOHNSON, *Appl. Phys. Lett.* **82** (2003) 1030.
16. A. INOUE and X. M. WANG, *Acta Mater.* **48** (2000) 1383.
17. A. INOUE, T. NEGISHI, H. KIMURA and T. AOKI, *Mater. Trans. JIM* **38** (1997) 185.

18. A. INOUE, T. AOKI and H. KIMURA, *ibid.* **38** (1997) 175.
19. W. H. WANG *et al.*, *Intermetallics* **10** (2002) 1249.
20. S. YI, J. K. LEE, W. T. KIM and D. H. KIM, *J. Non-Cryst. Solids* **291** (2001) 132.
21. A. INOUE, A. MURAKAMI, T. ZHANG and A. TAKEUCHI, *Mater. Trans. JIM* **38** (1997) 189.
22. S. YI, T. G. PARK and D. H. KIM, *J. Mater. Res.* **15** (2000) 2425.
23. B. SHEN and A. INOUE, *Mater. Trans.* **43** (2002) 1235.
24. D. Q. ZHAO, Y. ZHANG, M. X. PAN and W. H. WANG, *Mater. Trans. JIM* **41** (2000) 1427.
25. T. ZHANG, T. YAMAMOTO and A. INOUE, *Mater. Trans.* **43** (2002) 3222.
26. G. J. FAN *et al.*, *Appl. Phys. Lett.* **75** (1999) 2984.
27. C. L. QIN *et al.*, *Mater. Trans.* **44** (2003) 1042.
28. H. MEN, Z. Q. HU and J. XU, *Scripta Mater.* **46** (2002) 699.
29. A. INOUE, T. SHIBATA and T. ZHANG, *Mater. Trans. JIM* **36** (1995) 1420.
30. N. MITROVIC, S. ROTH and J. ECKERT, *Appl. Phys. Lett.* **78** (2001) 2145.
31. L. Q. MA, L. WANG, T. ZHANG and A. INOUE, *Mater. Res. Bullet.* **34** (1999) 915.
32. A. INOUE and B. SHEN, *Mater. Trans.* **43** (2002) 1230.
33. D. W. XING *et al.*, *T. Nonferr. Metal. Soc.* **13** (2003) 68.
34. T. ITOI and A. INOUE, *Mater. Trans. JIM* **41** (2000) 1256.
35. Q. S. ZHANG *et al.*, *Scripta Mater.* **49** (2003) 273.
36. E. S. PARK, H. K. LIM, W. T. KIM and D. H. KIM, *J. Non-Cryst. Solids* **298** (2002) 15.
37. J. F. SUN *et al.*, *T. Nonferr. Trans.* **13** (2003) 64.
38. T. ZHANG and A. INOUE, *Mater. Trans. JIM* **39** (1998) 1001.
39. Y. ZHANG *et al.*, *ibid.* **41** (2000) 1410.
40. T. ZHANG, K. KUROSAKA and A. INOUE, *ibid.* **42** (2001) 2042.
41. Z. P. LU, C. T. LIU and W. D. PORTER, *Appl. Phys. Lett.* **83** (2003) 2581.
42. Z. P. LU and C. T. LIU, *J. Mater. Res.* **19** (2004) 92.
43. Y. HU *et al.*, *Mater. Lett.* **57** (2003) 2698.
44. C. T. LIU, L. M. PIKE and N. G. CHEN, *Mater. Res. Soc. Symp. Proc.* **554** (1999) 305.
45. O. N. SENKOV and D. B. MIRACLE, *Mater. Res. Bullet.* **36** (2001) 2183.
46. A. GEBERT, J. ECKERT and L. SCHULTZ, *Acta Mater.* **46** (1998) 5475.
47. T. D. SHEN and R. B. SCHWARZ, *Appl. Phys. Lett.* **75** (1999) 49.
48. X. H. LIN, W. L. JOHNSON and W. K. RHIM, *Mater. Trans. JIM* **38** (1997) 473.
49. Z. P. LU and C. T. LIU, *Acta Mater.* **50** (2002) 3501.
50. D. J. SORDELET *et al.*, *Appl. Phys. Lett.* **83** (2003) 69.
51. Z. P. LU and C. T. LIU, *Phys. Rev. Lett.* **91** (2003) 115505.
52. M. H. RICHMAN, "An Introduction to Physical Metallurgy" (Blaisdell, Massachusetts, 1967) p. 215.
53. F. R. DE BOER, R. BOOM, W. C. M. MATTERNS, A. R. MIEDEMA and A. K. NIESSEN, "Cohesion in Metals" (North-Holland, Amsterdam, 1988).
54. E. MATSUBARA *et al.*, *Mater. Trans. JIM* **31** (1990) 228.
55. E. MATSUBARA *et al.*, *ibid.* **3** (1992) 873.
56. E. MATSUBARA *et al.*, *J. Non-Cryst. Solids* **150** (1992) 873.
57. H. TANAKA, *J. Phys. Condens. Mater.* **15** (2003) L491.
58. O. KUBASCHEWSKI and C. B. ALCOCK, "Metallurgical Thermochemistry" (Pergamon, Oxford, 1979).
59. A. INOUE and G. S. GOOK, *Mater. Trans. JIM* **36** (1995) 1180.
60. H. TAN *et al.*, *Acta Mater.* **51** (2003) 4551.